ADVANCES IN ATMOSPHERIC SCIENCES, VOL. 20, NO. 4, 2003, PP. 530–539

Remote Sensing Parameterization of Land Surface Heat Fluxes over Arid and Semi-arid Areas

MA Yaoming*[1,2] (马耀明), WANG Jiemin[1] (王介民), HUANG Ronghui[3] (黄荣辉), WEI Guoan[1](卫国安), Massimo MENENTI[4], SU Zhongbo[4] (苏中波), HU Zeyong[1] (胡泽勇), GAO Feng[1] (高 峰), and WEN Jun[4] (文 军)

[1] *Cold and Arid Regions Environmental and Engineering Research Institute, Chinese Academy of Sciences, Lanzhou* 730000

[2] *Institute of Tibetan Plateau Research, Chinese Academy of Sciences, Beijing* 100029

[3] *Institute of Atmospheric Physics, Chinese Academy of Sciences, Beijing* 100029

[4] *Alterra Green World Research, Wageningen UR*, 6700 *AA, Wageningen, The Netherlands*

(Received July 28, 2002; revised March 17, 2003)

ABSTRACT

Dealing with the regional land surfaces heat fluxes over inhomogeneous land surfaces in arid and semi-arid areas is an important but not an easy issue. In this study, one parameterization method based on satellite remote sensing and field observations is proposed and tested for deriving the regional land surface heat fluxes over inhomogeneous landscapes. As a case study, the method is applied to the Dunhuang experimental area and the HEIFE (Heihe River Field Experiment, 1988–1994) area. The Dunhuang area is selected as a basic experimental area for the Chinese National Key Programme for Developing Basic Sciences: Research on the Formation Mechanism and Prediction Theory of Severe Climate Disaster in China (G1998040900, 1999–2003). The four scenes of Landsat TM data used in this study are 3 June 2000, 22 August 2000, and 29 January 2001 for the Dunhuang area and 9 July 1991 for the HEIFE area. The regional distributions of land surface variables, vegetation variables, and heat fluxes over inhomogeneous landscapes in arid and semi-arid areas are obtained in this study.

Key words: land surface heat flux, arid and semi-arid area, Landsat TM, field observation

1. Introduction

The study on the energy exchanges between the land surface and atmosphere is of paramount importance for arid and semi-arid areas, e.g., the HEIFE (Heihe River Field Experiment) area and Dunhuang areas in northwestern China. Oasis, Gobi, sand desert, and mountains are distributed in the experimental areas. In other words, the experimental areas are typical inhomogeneous land surfaces. Some interesting detailed studies concerning the land surface heat fluxes over the two areas have been reported (Tsukamoto et al., 1992; Tsukamoto et al., 1995; Mitsuta et al., 1995; Hu et al., 1994; Maitani et al., 1995; Zhang et al., 2001 and Hu et al., 2002). This research was, however, on a point level or a local-patch level. Since the areal, and not only point-wise, information of land-surface atmosphere interaction is required, the aggregation of the individual results into a regional scale is necessary. Remote sensing from satellites offers the possibility to derive regional distribution of land surface heat fluxes.

The purpose of this study is to upscale the point or patch scale field observations of land surface variables and land surface heat fluxes to a regional distribution of them by using Landsat TM data and field observations.

2. Landsat TM data and field observation data

The Landsat-5 Thematic Mapper (TM) and Landsat-7 Thematic Mapper provide a spectral radi-

*E-mail: ymma@ns.lzb.ac.cn

ance in seven narrow bands, with a spatial resolution of about 30×30 m^2 for three visible bands (Band 1, 2, 3) and three near-infrared bands (Band 4, 5, 7), and 120×120 m^2 for the thermal infrared band 6 of Landsat-5 TM and 60×60 m^2 for the thermal infrared band 6 of Landsat-7 TM. The four TM images used in this paper are at 1000 LST 3 June 2000 (beginning of summer), 22 August 2000 (end of summer), and 29 January 2001 (winter) over the Dunhuang area, and 1000 LST 7 July 1991 over the HEIFE area.

The most relevant data, collected at Dunhuang and the HEIFE surface stations to support the parameterization of land surface heat fluxes and analysis of TM images, consist of surface radiation budget components, surface radiation temperature, surface reflectance, vertical profiles of air temperature, humidity, wind speed, and direction measured at the PBL towers, Sodar, radiosonde, tether-sonde and turbulent fluxes measured by the eddy-correlation technique, soil heat flux, soil temperature profiles, soil moisture profiles, and the vegetation state.

3. Theory and scheme

By combining satellite remote sensing (e.g., Landsat TM data) with field observations, the land surface heat fluxes over an inhomogeneous land surface can be derived. The general concept of the methodology is shown in Fig. 1.

3.1 *Net radiation*

The regional net radiation flux can be derived from:

$$R_{\rm n}(x,y) = [1 - r_0(x,y)]K_{\downarrow}(x,y) + L_{\downarrow}(x,y) - \varepsilon_0(x,y)\sigma T_{\rm sfc}^4(x,y)\ , \quad (1)$$

where $r_0(x,y)$ is surface reflectance. It can be derived from Landsat TM data using a four- stream radiative transfer assumption for atmospheric correction in solar spectral bands (Vehoef, 1997; Ma, 2001). Surface temperature $T_{\rm sfc}(x,y)$ in Eq.(1) can be derived from Landsat TM band-6 (10.2–12.5 μm) spectral radiance (Ma, 2001). The incoming short wave radiation flux and incoming long wave radiation flux $K_{\downarrow}(x,y)$ and $L_{\downarrow}(x,y)$ in Eq.(1) can be derived from the radiative transfer model MODTRAN (Ma, 2001). Surface emissivity $\varepsilon_0(x,y)$ is determined by Valor and Caselles's method (1997):

$$\begin{aligned}\varepsilon_0(x,y) =& \varepsilon_{\rm v}(x,y)P_{\rm v}(x,y) \\ &+ \varepsilon_{\rm g}(x,y)[1 - P_{\rm v}(x,y)] \\ &+ 4 < \varepsilon > [1 - P_{\rm v}(x,y)]P_{\rm v}(x,y)\ , \end{aligned} \quad (2)$$

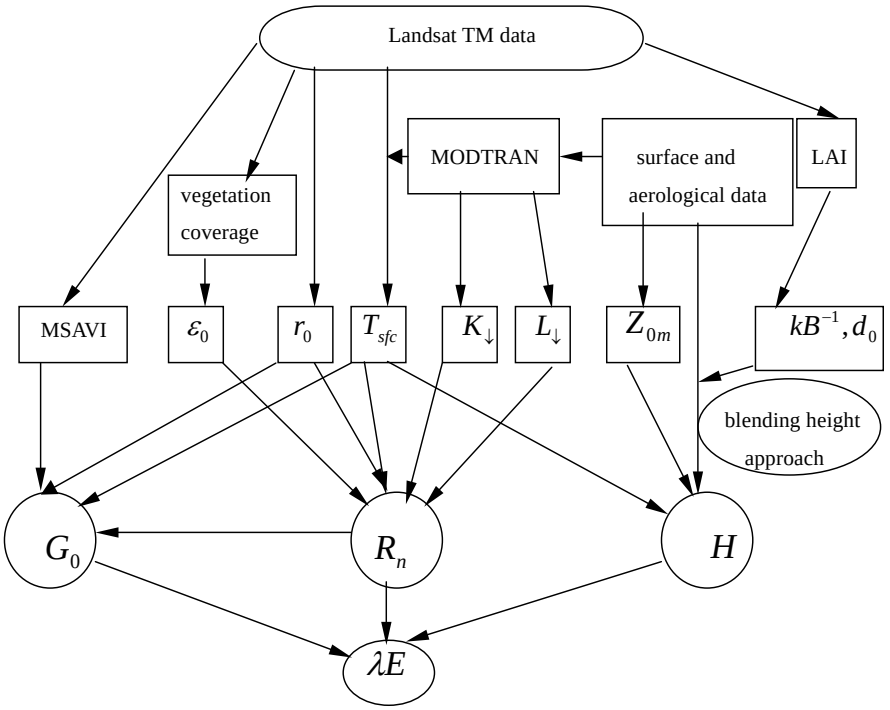

Fig. 1. Diagram of the parameterization procedure by combining Landsat TM data with field observations.

and vegetation coverage by Carlson and Ripley (1997):

$$P_{\rm v}(x,y)=\left[\frac{I_{\rm NDV}(x,y)-I_{\rm NDVmin}}{I_{\rm NDVmax}-I_{\rm NDVmin}}\right]^2 , \qquad (3)$$

where $I_{\rm NDV}$ is the Normalized Difference Vegetation Index (NDVI) and $I_{\rm NDVmin}$ and $I_{\rm NDVmax}$ are the NDVI values for bare soil and full vegetation respectively.

3.2 *Soil heat flux*

The regional soil heat flux $G_0(x,y)$ is determined using a parameterization based on Modified Soil Adjusted Vegetation Index (MSAVI, $I_{\rm MSAV}$, Qi et al., 1994):

$$\begin{aligned}G_0(x,y)=&\,R_{\rm n}(x,y)[T_{\rm sfc}(x,y)/r_0(x,y)]\\&\times(a+b\overline{r}_0+c\overline{r}_0^2)[1+dI_{\rm MSAV}(x,y)^e] ,\end{aligned} \qquad (4)$$

where the constants $a,b,c,d,$ and e are determined from field data observed at the HEIFE and Dunhuang observation stations; $\overline{r}_0$ is a daily mean reflectance value, i.e. for the HEIFE case:

$$\begin{aligned}G_0(x,y)=&\,R_{\rm n}(x,y)\frac{T_{\rm sfc}(x,y)}{r_0(x,y)}(0.00025+0.00436\overline{r}_0\\&+0.00845\overline{r}_0^2)[1-0.979I_{\rm MSAV}(x,y)^4] .\end{aligned} \qquad (5)$$

For the Dunhuang case:

$$\begin{aligned}G_0(x,y)=&\,R_{\rm n}(x,y)\frac{T_{\rm sfc}(x,y)}{r_0(x,y)}(0.00028+0.00424\overline{r}_0\\&+0.00875\overline{r}_0^2)[1-0.982I_{\rm MSAV}(x,y)^4] ,\end{aligned} \qquad (6)$$

where

$$I_{\rm MSAV}(x,y)=\frac{2r_4(x,y)+1-\sqrt{[2r_4(x,y)+1]^2-8[r_4(x,y)-r_3(x,y)]}}{2} \qquad (7)$$

where r_3 and r_4 are the band reflectance of Landsat TM Band-3 and Band-4 on the land surface.

3.3 *Sensible heat flux*

The regional distribution of sensible heat flux can be estimated from

$$H(x,y)=\rho c_p k^2 u(x,y)\frac{[T_{\rm sfc}(x,y)-T_a(x,y)]}{\left[\ln\dfrac{z-d_0(x,y)}{Z_{0m}(x,y)}+kB^{-1}(x,y)-\psi_h(x,y)\right]\left[\ln\dfrac{z-d_0(x,y)}{Z_{0m}(x,y)}-\psi_m(x,y)\right]} . \qquad (8)$$

To simulate sensible heat flux on a large scale, a straightforward method is to scale-up or aggregate the regional sensible flux by a weighted average of the contributions from different surface elements, based on the principle of flux conservation. A method of "blending height" is proposed to derive the regional sensible heat flux in this study. If the local-scale advection is comparatively small during the period of Landsat TM observation, the development of convection boundary layer may adjust the surface-disorganized variability at "blending height" where the atmospheric characteristics become proximately independent of the horizontal position (Mason, 1988). Based on this approach, the regional sensible heat flux density $H(x,y)$ can be described as

$$H(x,y)=\rho c_p k^2 u_{\rm B}\frac{[T_{\rm sfc}(x,y)-T_a(x,y)]}{\left[\ln\dfrac{z_{\rm B}-d_0(x,y)}{Z_{0m}(x,y)}+kB^{-1}(x,y)-\psi_h(x,y)\right]\left[\ln\dfrac{z_{\rm B}-d_0(x,y)}{Z_{0m}(x,y)}-\psi_m(x,y)\right]} , \qquad (9)$$

where $Z_{\rm B}$ is the blending height and, $u_{\rm B}$ is the wind speed at the blending height. $Z_{\rm B}$ and $u_{\rm B}$ can be determined by field measurements or numerical models. In this study, they are determined with the aid of field measurements of radiosonde (Dunhuang area) and tethersonde and Sodar (HEIFE area). $T_{\rm a}(x,y)$ in Eq.(9) is the regional distribution of air temperature at the reference height. An improved interpolation method is proposed here to derive the regional distribution of air temperature over the oasis-desert system of HEIFE. In other words, the regional distribution of air temperature $T_{\rm a}(x,y)$ over the HEIFE area can be derived using this improved numerical interpolation method based on a number of field observations of air temperature and regional surface temperature as (Ma et al., 2002)

$$T_{\rm a}(x,y)=T_{\rm sfc}(x,y)-DT_{\rm a}(x,y) . \qquad (10)$$

The regional distribution of air temperature $T_{\rm a}(x,y)$

in the Dunhuang area can be simply derived from $T_{\text{a-oasis}}(x,y)$ and $T_{\text{a-Gobi-desert}}(x,y)$ due to only two kinds of surfaces (oasis and Gobi-desert) existing in Dunhuang area. The effective aerodynamic roughness length $Z_{0m}(x,y)$ in Eq.(9) over the HEIFE area, including the effect of topography, low vegetation (e.g. grass), and taller plants (e.g., wheat canopy, trees and shrubs), can be determined by Taylor's model (Taylor et al., 1989) since the surface conditions in the HEIFE area are the same as in Taylor's model. As for the effective aerodynamic roughness length $Z_{0m}(x,y)$ in the Dunhuang area, it can be simply derived from $Z_{0m-\text{oasis}}(x,y)$ and $Z_{0m-\text{Gobi-desert}}(x,y)$ due to only two kinds of surfaces (oasis and Gobi-desert) in the Dunhuang area. Raupach's method (Raupach, 1994) is used to derive the zero-plane displacement $d_0(x,y)$ in Eq.(9) over the HEIFE and Dunhuang areas, i.e.,

$$1-\frac{d_0(x,y)}{h(x,y)}=\frac{1-\exp(-\sqrt{c_{d1}I_{\text{LA}}(x,y)})}{\sqrt{c_{d1}I_{\text{LA}}(x,y)}}\,, \qquad (11)$$

where I_{LA} is the leaf area index (LAI), $h(x,y)$ is the height of vegetation and c_{d1} is a free parameter (Raupach, 1994). In other words, the zero-plane displacement $d_0(x,y)$ can be derived when LAI and the vegetation height are determined over the two areas. $kB^{-1}(x,y)$ in Eq.(9) is determined by using the relationship between $kB^{-1}(x,y)$ and $T_{\text{s}}(x,y)$, $\psi_h(x,y)$ and $\psi_m(x,y)$ in Eq.(9) are the integrated stability functions. They can be determined by using the models of Paulson (1970) and Webb (1970).

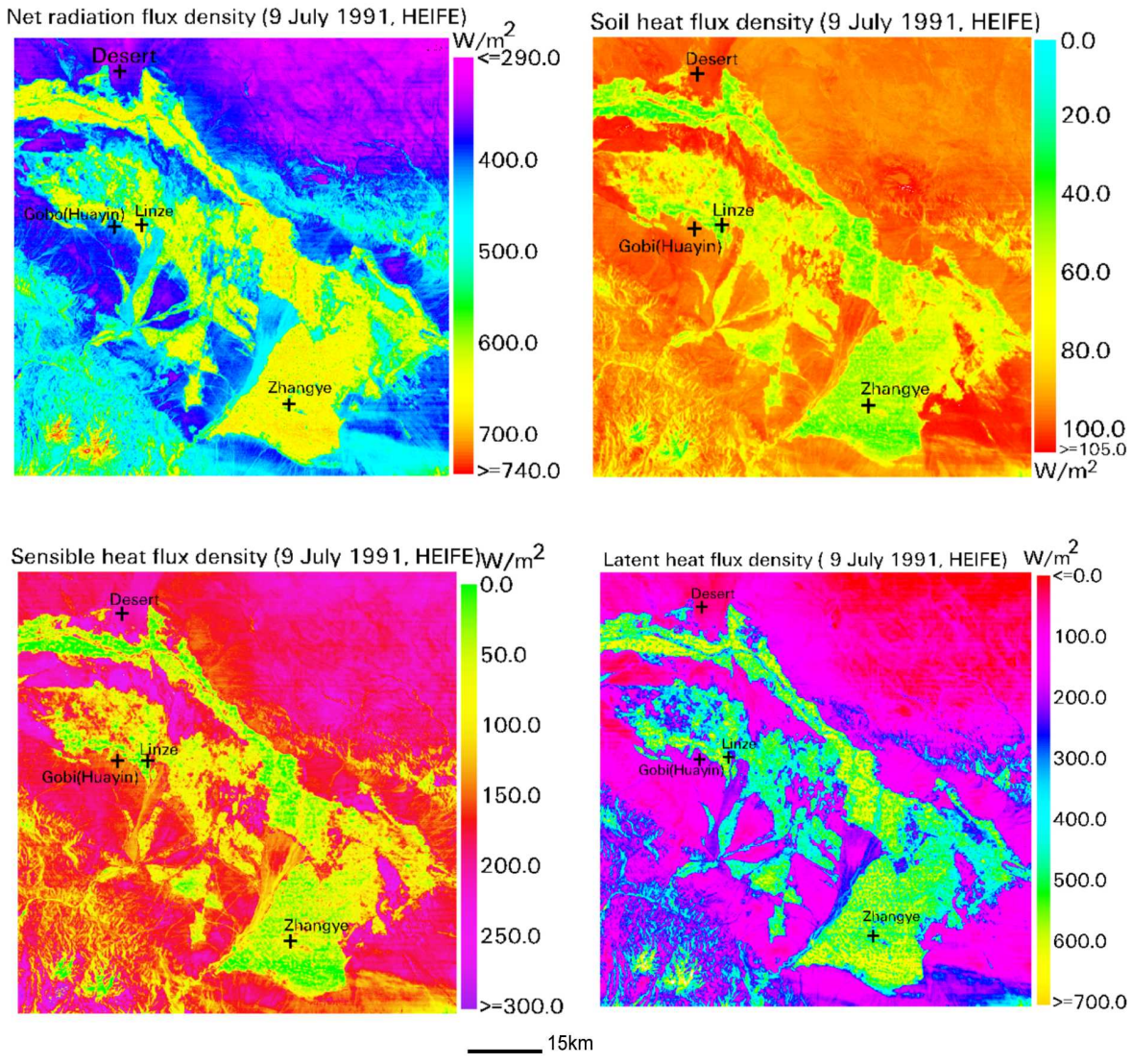

Fig. 2. Maps of land surface heat fluxes for the HEIFE area. 1000 LST, July 9, 1991.

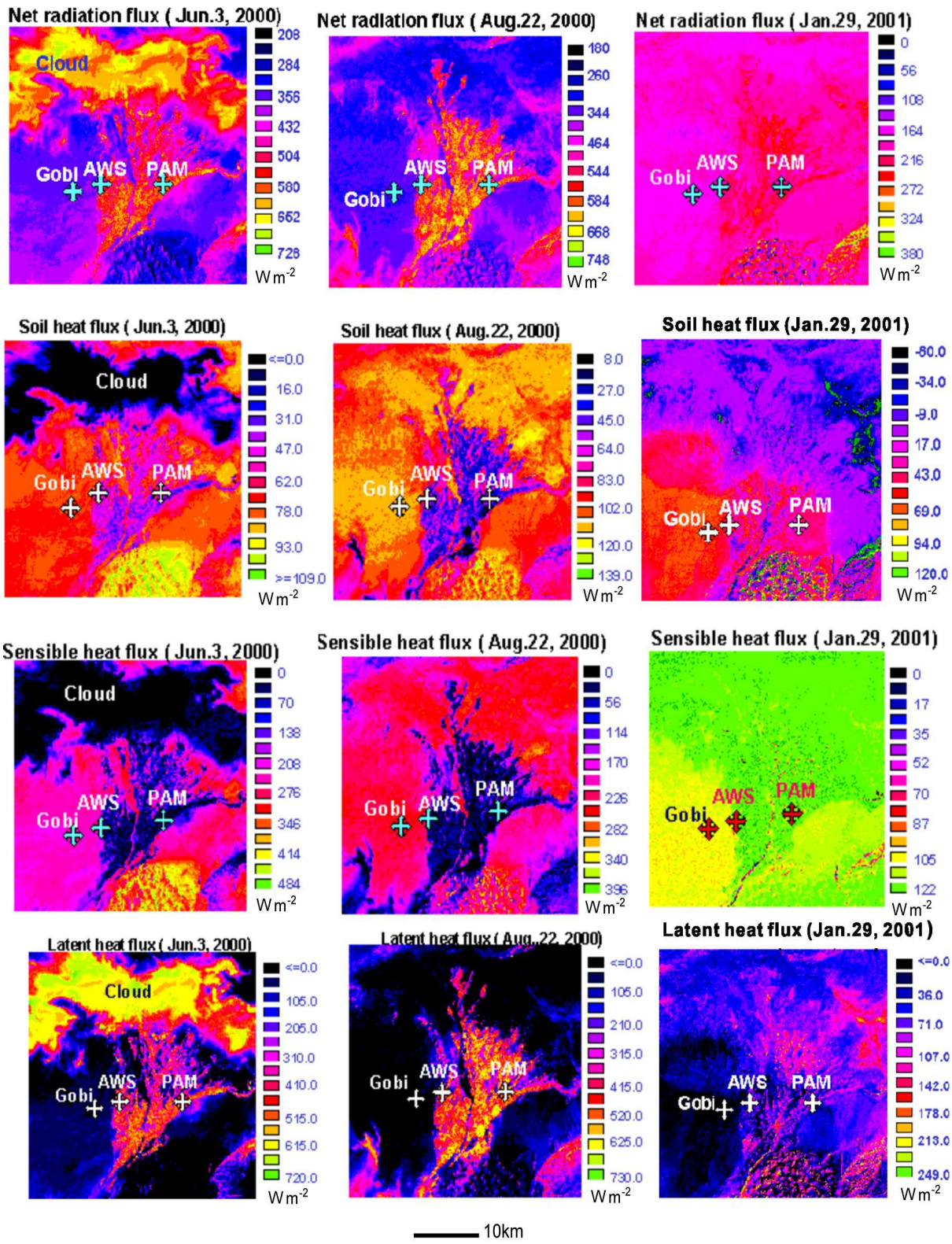

Fig. 3. Maps of land surface heat fluxes for the Dunhuang area. 1000 LST.

Table 1. The distribution range and peaks of land surface variables, vegetation variables, and land surface heat fluxes over the Dunhuang area

		Range	Oasis (peak)	Gobi desert (peak)
3 Jun 2000	NDVI	0.00–0.46	~ 0.30	~ 0.00
	MSAVI	0.00–0.40	~ 0.26	~ 0.00
	P_v	0.00–0.95	~ 0.28	~ 0.00
	r_0	0.10–0.30	~ 0.17	~ 0.22
	LAI	0.00–8.80	~ 1.80	~ 0.00
	T_{sfc}(°C)	2.0–63.0	~ 26.0	~ 48.0
	R_n (W m^{-2})	250–550	~ 520	~ 330
	G_0 (W m^{-2})	1–105	~ 36	~ 74
	H (W m^{-2})	2–405	~ 50	~ 245
	λE (W m^{-2})	0–520	~ 450	~ 50
22 Aug 2000	NDVI	0.00–0.74	~ 0.64	~ 0.06
	MSAVI	0.00–0.65	~ 0.50	~ 0.00
	P_v	0.02–0.98	~ 0.85	~ 0.02
	r_0	0.08–0.36	~ 0.14	~ 0.23
	LAI	0.00–8.80	~ 2.10	~ 0.00
	T_{sfc}(°C)	5.0–57.0	~ 15.0	~ 49.0
	R_n (W m^{-2})	260–660	~ 600	~ 330
	G_0 (W m^{-2})	15–120	~ 40	~ 103
	H (W m^{-2})	0–300	~ 30	~ 230
	λE (W m^{-2})	–20–650	~ 550	~ 30

Table 2. The distribution range and peaks of land surface variables, vegetation variables, and land surface heat fluxes over the HEIFE area (9 July 1991)

	Range	Oasis (peak)	Gobi desert (peak)
NDVI	0.10–0.75	~ 0.66	~ 0.15
MSAVI	0.08–0.92	~ 0.80	~ 0.25
P_v	0.00–0.95	~ 0.78	~ 0.20
r_0	0.04–0.30	~ 0.12	~ 0.26
LAI	0.00–5.80	~ 2.80	~ 0.45
T_{sfc}(°C)	5.0–55.0	~ 16.0	~ 44.0
R_n (W m^{-2})	290–750	~ 650	~ 380
G_0 (W m^{-2})	30–105	~ 50	~ 90
H (W m^{-2})	0–300	~ 90	~ 230
λE (W m^{-2})	0–700	~ 500	~ 100

3.4 *Latent heat flux*

The regional latent heat flux $\lambda E(x, y)$ is derived as the residual of the energy budget theorem for the land surface, i.e.,

$$\lambda E(x, y) = R_n(x, y) - H(x, y) - G_0(x, y) . \quad (12)$$

4. Case study and validation

Figures 2 and 3 show the distribution maps of land surface heat fluxes over the HEIFE area and Duhuang areas. The frequency distributions of land surface fluxes over the two areas are shown in Fig. 4. The derived land surface heat fluxes are validated by field measurements. In Fig. 5, the derived results are plotted against the measured values in the fields of Dunhuang and the HEIFE for four terms of the energy balance. The 1:1 line is also plotted in the graphs. The land surface heat fluxes, which were derived from SEBAL (Wang et al., 1995; Ma et al., 1999), are plotted in Fig. 5 as well. Since it is difficult to determine where the exact locations of the experimental sites are, the values of a 5×5 pixel rectangle, surrounding the determined Universal Transverse Mercator (UTM) coordinate, are compared with the field measurements.

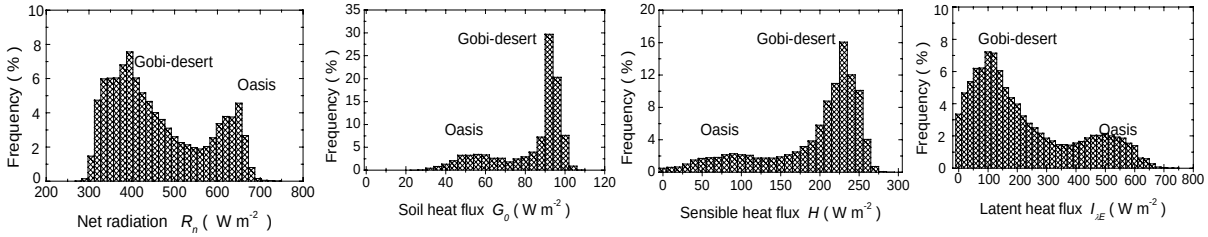

(a)

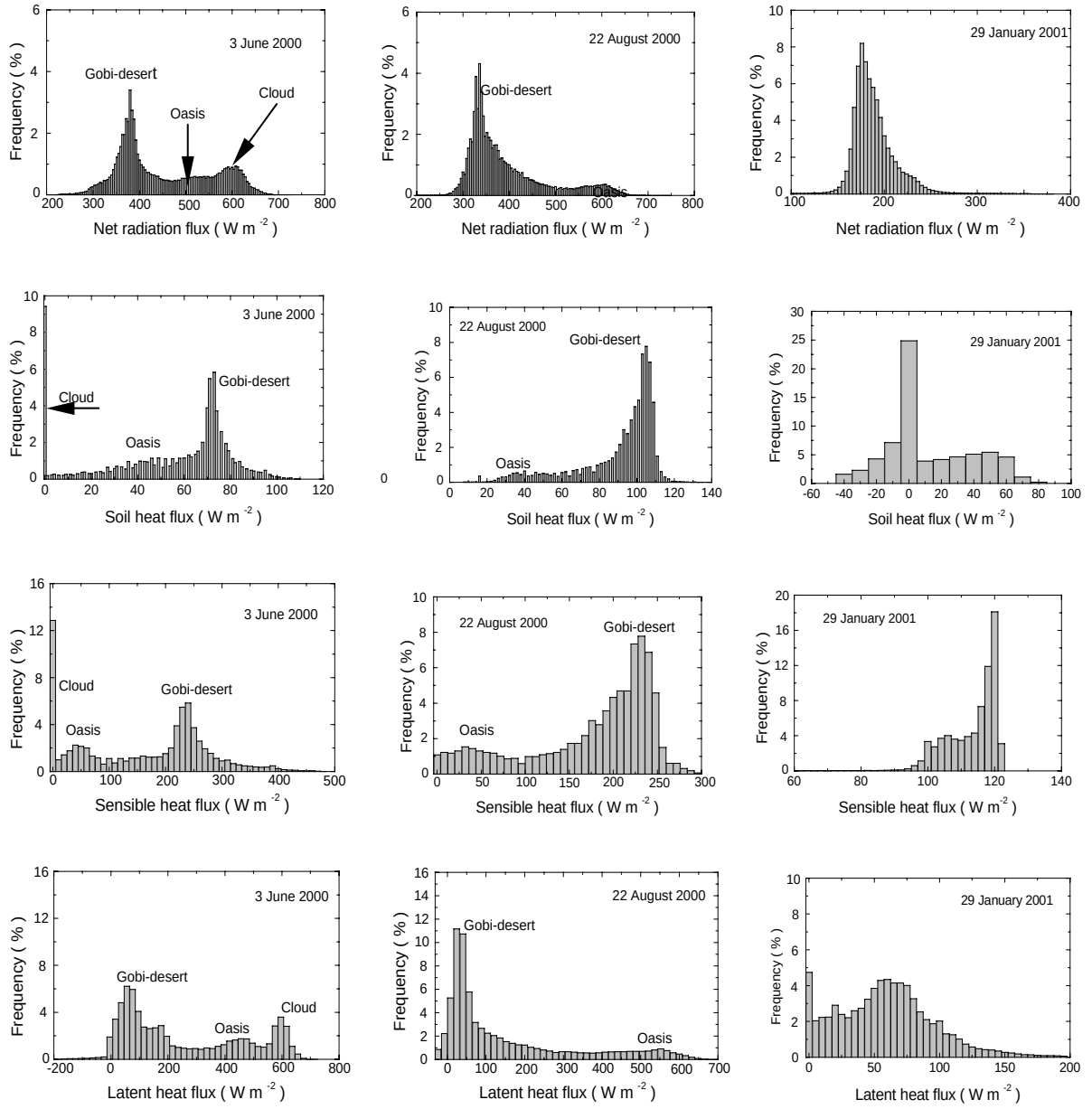

(b)

Fig. 4 Frequency distribution of land surface heat fluxes. (a) HEIFE; (b) Dunhuang.

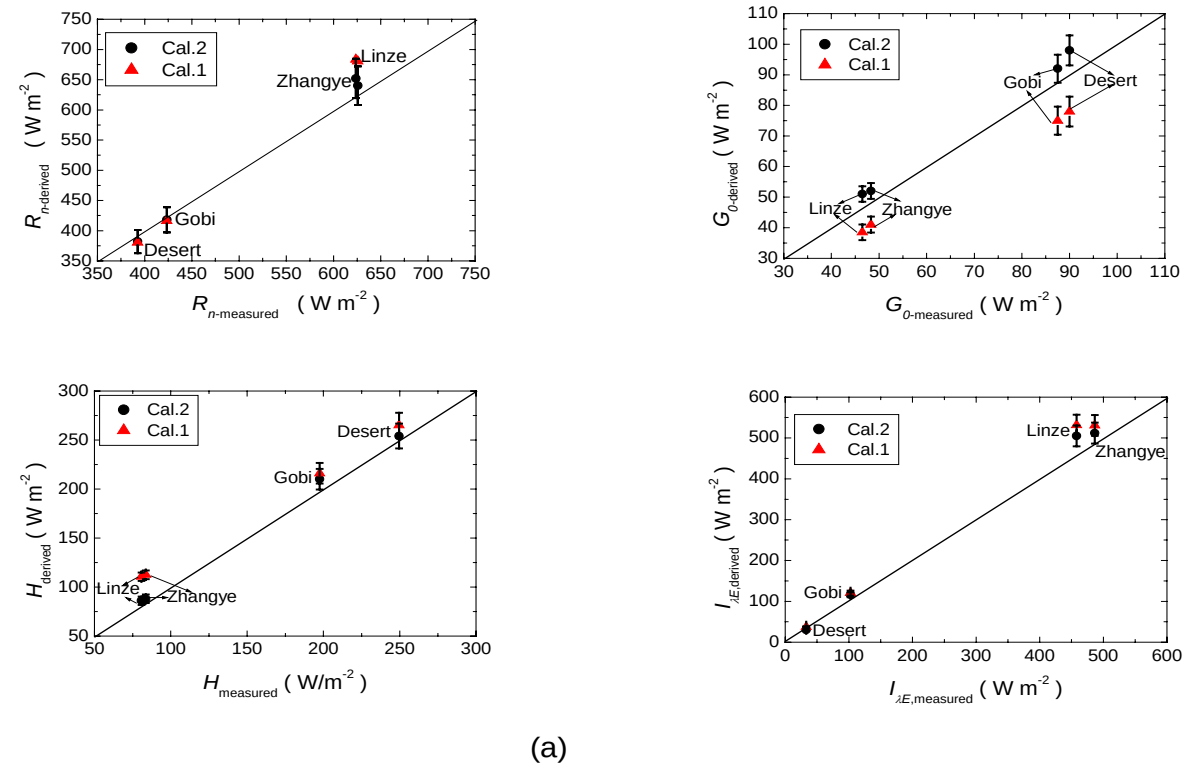

(a)

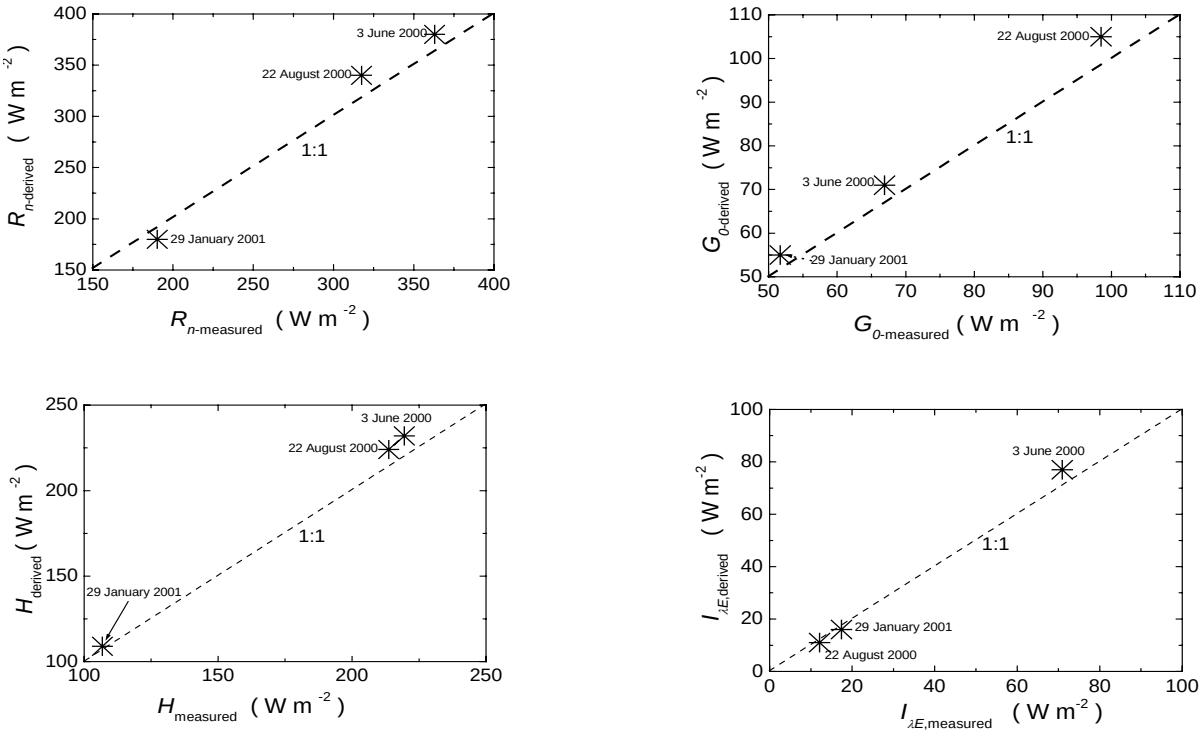

(b)

Fig. 5 Validation of the derived results against the field measurements for land surface heat fluxes, together with the 1:1 line. Cal.1: former results (Wang et al., 1995; Ma et al., 1999); Cal.2: this research. (a) HEIFE; (b) Duhuang.

The mean absolute percent difference (MAPD, $D_{\rm MAP}$) can quantitatively measure the difference between the derived results ($H_{\rm derived(}_{i}_{\rm)}$) and measured values ($H_{\rm measured(}_{i}_{\rm)}$):

$$D_{\rm MAP} = \frac{100}{n}\sum_{i=1}^{n}\left(\frac{\mid H_{\rm derived(}_{i}_{\rm)} - H_{\rm measured(}_{i}_{\rm)} \mid}{H_{\rm measured(}_{i}_{\rm)}}\right) . \tag{13}$$

The results show that: (1) the derived land surface variables (land surface reflectance and surface temperature), vegetation variables (NDVI, MSAVI, vegetation coverage $P_{\rm v}$ and LAI, and land surface heat fluxes (net radiation flux $R_{\rm n}$, soil heat flux G_0, sensible heat flux H, and latent heat flux λE) over two case study areas are in good accordance with the land surface status. These parameters in summer show a wide range due to the strong contrast of surface features during this season, and there are two peaks in the figures of all distribution maps and all frequency distributions histograms. The first ones correspond to oasis and the other peak corresponds to the Gobi desert (see Table 1 and Table 2). Although there are differences between oasis and Gobi desert for land surface variables, vegetation variables, and land surface heat fluxes over the two areas in winter, they are not clear; (2) the derived surface reflectance and surface temperature in this research are in good accordance with the field measurements, and they are better than the results derived from the regression relationship (Wang et al., 1995; Ma et al., 1999) with MAPD (mean absolute percent difference) less than 10%; (3) the derived net radiation fluxes over the two areas are very close to the field measurements with MAPD less than 7%; (4) the parameterization method based on MSAVI for soil heat flux is suitable for the inhomogeneous land surface of arid and semi-arid areas. Although the derived regional soil heat flux is slightly higher than the measured value, the MAPD gets smaller than the former derived value based on the NDVI (Wang et al., 1995; Ma et al., 1999); (5) the derived regional sensible heat fluxes with MAPD of around 6% at five validation sites in Dunhuang and HEIFE are in good agreement with the field measurements; (6) the derived regional latent heat flux, which is based on the energy balance equation, is acceptable for the whole HEIFE area and Dunhuang area; and (7) net radiation flux and latent heat flux in summer (June and August) are much higher than in winter over the oasis area of Dunhuang, but the sensible heat flux is much lower than in winter. Net radiation flux, sensible heat flux, and soil heat flux are much higher in summer than in winter over Gobi desert area of Dunhuang, and latent heat flux over the the Gobi desert is very low in summer ($\sim$40 W m^{-2}). This is caused by the seasonal difference and land surface status difference between summer and winter.

5. Concluding remarks

In this study, the regional distributions of land surface variables (surface reflectance and surface temperature), vegetation variables (NDVI, MSAVI, vegetation coverage, and LAI) and land surface heat fluxes (net radiation, soil heat flux, and sensible and latent heat flux) over the inhomogeneous areas of Dunhuang and HEIFE are derived with the aid of Landsat TM data and field observations. Compared with previous studies (Wang et al., 1995; Ma et al., 1999), the new method has been proved to be a better approach for getting related air-land parameters over heterogeneous landscape due to the improvements in old parameterizations (Wang et al., 1995; Ma et al., 1999). This study forms a sound basis to study land surface variables, vegetation variables, and land surface fluxes over inhomogeneous landscapes.

The vegetation variables cannot be validated in this research due to the lack of such measurements during the HEIFE and Dunhuang experiments. In future experiments, more attention should be paid to the measurements of vegetation variables, such as NDVI, LAI, and vegetation coverage.

Acknowledgments. This work was under the auspices of the Innovation Project of the Chinese Academy of Sciences (KZCX3-SW-329), the Chinese National Key Programme for Developing Basic Sciences (G1998040900), and the National Natural Science Foundation of China (40275003). Some parts of this study were done as cooperative research works in the Disaster Prevention Research Institute, Kyoto University, and the Alterra Green World Research, Wageningen UR, the Netherlands. The authors wish to acknowledge Profs. H. Ishikawa, O. Tsukamoto, M. Maitani, and E. Ohtaki for their kind help and useful discussions.

REFERENCES

Carlson, T. N., and D. A. Ripley, 1997: On the relation between NDVI, fractional vegetation cover, and leaf area index. *Remote Sens. Environ.*, **62**, 241–252.

Hu Yinqiao, Gao Youxi, Wang Jiemin, Ji Guoliang, Shen Zhibao, Cheng Linsheng, Chen Jiayi, and Li Shouqian, 1994: Some achievements in scientific research during HEIFE. *Plateau Meteorology*, **13**(3), 225–236. (in Chinese)

Hu Zeyong, Huang Ronghui, Wei Guoan, and Gao Huangcun, 2002: Variations of surface atmospheric variables and energy budget during a sandstorm passing Dunhuang on June 6 of 2000. *Chinese Journal of Atmospheric Sciences*, **26**(1), 1–8. (in Chinese)

Ma Yaoming, Wang Jiemin, M. Menenti, and W. G. M. Bastiaanssen, 1999: Estimation of fluxes over the heterogeneous land surface with the aid of satellite remote sensing and field observation. *Acta Meteor. Sinica*, **57**(2), 180–189. (in Chinese)

Ma, Y., 2001: Parameterization of land surface heat flux densities over inhomogeneous landscape by combining satellite remote sensing with field observations. Ph. D dissertation, Okayama University, Japan, 195pp.

Ma, Y., O. Tsukamoto, H. Ishikawa, Z. Su, M. Menenti, J. Wang, and J. Wen, 2002: Determination of regional land surface heat flux densities over heterogeneous landscape of HEIFE Integrating satellite remote sensing with field observations. *J. Meteor. Soc. Japan*, **80**(3) 485–501.

Maitani, T., K. Sahashi, E. Ohtaki, O. Tsukamoto, and Y. Mitsuta, 1995: Measurements of turbulent fluxes and model simulation of micrometeorology in a wheat field at Zhangye oasis. *J. Meteor. Soc. Japan*, **73**(5): 959–965.

Mason, P., 1988: The formation of areally averaged roughness lengths. *Quart. J. Roy. Meteor. Soc.*, **114**, 399–420.

Mitsuta, Y., I. Tamagawa, K. Sahashi, and J. Wang, 1995: Estimation of annual evaporation from the Linze desert during HEIFE. *J. Meteor. Soc. Japan*, **73**(5), 967–974.

Paulson, C. A., 1970: The mathematical representation of wind speed and temperature profiles in the unstable atmospheric surface layer. *J. Appl. Meteor.*, **9**, 857–861.

Qi, J., A. Chehbouni, A. R. Huete, Y. H. Kerr, and S. Sorooshian, 1994: A modified soil adjusted vegetation index. *Remote Sens. Environ.*, **48**, 119–126.

Raupach, M. R., 1994: Simplified expressions for vegeta tion roughness length and zero-plane displacements as functions of canopy height and area index. *Bound.-Layer Meteor.*, **71**, 211–216.

Taylor, P. A., R. I. Sykes, and P. J. Mason, 1989: On the parameterization of drag over small scale topography in neutrally stratified boundary flow. *Bound.-Layer Meteor.*, **48**, 409–422.

Tsukamoto, O., J. Wang, and Y. Mitsuta, 1992: A significant evening peak of vapour pressure at an oasis in the semi-arid region. *J. Meteor. Soc. Japan*, **70**(6), 1155–1159.

Tsukamoto, O., K. Sahashi, and J. Wang, 1995: Heat budget and evapotranspiration at an oasis surface surrounded by desert. *J. Meteor. Soc. Japan*, **73**(5), 925–935.

Valor, E., and V. Caselles, 1997: Mapping land surface emissivity from NDVI: Application to European, African, and South American areas. *Remote Sens. Environ.*, **57**, 167–184.

Verhoef, W., 1997: Theory of radiative transfer models applied in optical remote sensing of vegetation canopies. Ph. D. dissertation, Remote Sensing Department of National Aerospace Laboratory, The Netherlands.

Wang, J., Y. Ma, M. Menenti, W. G. M. Bastiaanssen, and Y. Mitsuta, 1995: The scaling-up of processes in the heterogeneous landscape of HEIFE with the aid of satellite remote sensing. *J. Meteor. Soc. Japan.*, **73**(6), 1235–1244.

Webb, E. K., 1970: Profile relationships: The log-linear range and extension to strong stability. *Quart. J. Roy. Meteor. Soc.*, **96**, 67–90.

Zhang Qiang, Wei Guoan, and Huang Ronghui, 2001: Bulk transfer coefficients of momentum and sensible heat over the Gobi desert surface in north-western arid area. *Science in China* (*Series D*), **31**(9), 783–792. (in Chinese)

干旱及半干旱地区地表能量通量的卫星遥感参数化

马耀明　王介民　黄荣辉　卫国安　Massimo Menenti　苏中波　胡泽勇　高 峰　文 军

摘　要

对干旱及半干旱地区非均匀地表区域地表能量通量的研究是一个十分重要但又是一个难点问题。作者提出了一个基于卫星遥感和地面观测的参数化方案，并把其用于中国西北地区“我国重大气候和天气灾害形成和预测理论的研究”(国家重点基础研究发展规划项目G1998040900, 1999–2003)的“敦煌试验” 区和“黑河试验”(HEIFE, 1989–1994)区，并利用4个景(“敦煌试验区”：2000年6月3日–初夏、2000年8月22日–夏末和2001年1月29日–冬天；“黑河试验”区：1991年7月9日–夏季）的陆地资源卫星Landsat–5 TM 和Landsat–7 TM资料进行了分析研究，得到了有关干旱及半干旱地区非均匀地表区域地表特征参数、植被参数和地表能量通量的分布图像。最后还讨论了参数化方案的适用范围和需改进之处.

关键词: 区域能量通量, 干旱及半干旱地区, Landsat TM, 地面观测